Monte Carlo simulation of an Ising model on a Sierpiński carpet

G. Pruessner,* D. Loison,† and K. D. Schotte‡
Institut für Theoretische Physik, Freie Universität Berlin, Arnimallee 14, 14195 Berlin, Germany
(Received 1 February 2000; revised manuscript received 18 December 2000; published 12 September 2001)

We study by Monte Carlo simulation the equilibrium and dynamical critical properties of fractal lattices with noninteger Hausdorff dimension. These lattices are known to be good candidates to bridge the gap between integer dimensions. Focusing on the Sierpiński carpet with Ising spins, we are able to obtain the critical exponents that are to be compared to the predictions of the renormalization group. We point out that the use of finite-size scaling is forbidden for fractal lattices. This might explain the difference from the exponents obtained in previous studies.

DOI: 10.1103/PhysRevB.64.134414 PACS number(s): 75.10.−b, 05.70.Fh, 64.60.Cn, 75.40.Mg

I. INTRODUCTION

The understanding of phase transitions has been greatly improved by the introduction of the renormalization group (RG). In particular, various approaches such as that based on the nonlinear sigma model or the $d=4-\epsilon$ Wilson expansion make predictions regarding the critical behavior of systems for noninteger space dimensions. In contrast to integer dimensions, it seems to be impossible to verify these predictions on critical exponents for second-order phase transitions with numerical simulations. This is regrettable because some systems, like the Potts model[1] or frustrated-spin models,[2] are predicted to change their behavior from second order to first order at specific noninteger dimensions.

An effective noninteger dimension and effective critical exponents that differ from their standard values are expected in partially finite systems undergoing a phase transition. Ising systems, which are finite in all, say d, but one dimension, have been studied by numerical transfer-matrix methods.[3,4] The effective spatial dimension, as defined by the finite-size scaling of the longitudinal correlation length, can be tuned by changing the coupling constant at the boundaries of the finite layers. Depending on the value of this coupling, the boundary varies between periodic and antiperiodic. The resulting effective exponents agrees with the corresponding $4-\epsilon$ RG calculation at the effective spatial dimension. A similar attempt to study dimensional crossover has been undertaken, by means of RG, in the space $S^1\times R^{3-\epsilon}$,[5,6] where the circumference of S^1 has the finite value L. Two qualitatively different regimes are expected, depending on the ratio of L and the correlation length ξ. For $L/\xi\to\infty$ the model should behave as a $(4-\epsilon)$-dimensional model, while $L/\xi \to 0$ should lead to $(3-\epsilon)$-dimensional behavior. Again effective exponents can be calculated, which now depend directly on L. The main difference between these models and the model considered in this paper is that the former reach standard theories in the thermodynamic limit, where the transfer-matrix method recovers the model with (effective) dimension d, while the RG approach is supposed to lead to standard $4-\epsilon$ RG.

To overcome this problem, another way of scaling the effective spatial dimension has been implemented, again by using numerical transfer-matrix methods.[7,8,4] Here the connectivity of the lattice becomes a continuous parameter, varying between nearest-neighbor coupling and uncoupled one-dimensional chains. Extensive calculations have been carried out between effective dimension $d_{eff}=1$ and $d_{eff}=2$.[8] Although the system obtained by this procedure is translationally invariant, it remains open whether the interpolation scheme is capable of covering the thermodynamic limit. Moreover, the physical interpretation of the interpolation is not obvious.

Another suggestion, at the beginning of the 1980s, was to use fractal lattices to simulate systems in noninteger dimensions. However, as disordered systems, fractals are not translationally invariant and this causes difficulties for the simulations. Disorder can introduce relevant fields leading eventually to a new stable fixed point. In the case of fractals the situation is different: The lack of translational invariance is caused by an ordered removal of sites, which leads to a scale-invariant lattice. This fact makes fractal systems good candidates for being treated by RG techniques since they rely on rescaling. The prediction is that a fractal lattice possessing a noninteger dimension and infinite-ramification order[9,10] reaches the standard fixed points.

The lack of translational invariance is considered as problematic in analytic approaches, such as,[11,9] which were performed by means of low-temperature RG and Migdal-Kadanoff realspace RG,[12,13] respectively. The failure of a fractal to be translationally invariant is characterized by the topological property lacunarity, which basically measures the variance of the density of sites within the lattice.[14–16] At vanishing lacunarity, translational invariance is recovered. Therefore especially analytical techniques have been applied to systems of low lacunarity.[17,18] However, studies on such lattices suffer for their large lateral size of the initiator,[18] which is needed in order to distribute the holes evenly (see Sec. II).

In this paper we consider solely the influence of the noninteger dimension of the fractal lattices. We have chosen the Sierpiński carpet (see Fig. 1) as a fractal. Previous Monte Carlo simulations[19–21] with Ising spins on this lattice have produced controversial results partly due to limited computing power available. There is also a methodological problem with the finite-size scaling approach used, which we will show is inapplicable to fractal lattices. For comparison, our results for the critical properties based on equilibrium Monte

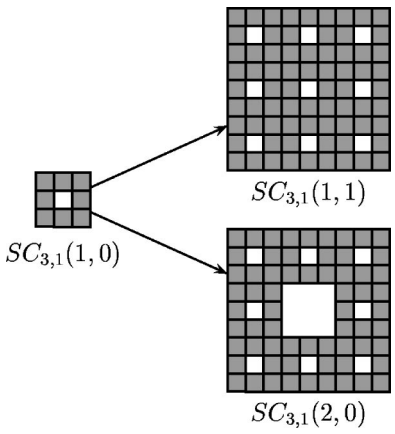

FIG. 1. Different ways of enlarging a Sierpiński carpet: The upper one is ''expanded,'' the lower one ''iterated.''

Carlo methods are checked using short-time dynamic Monte Carlo.[22–25]

The outline of the paper is the following. In Sec. II we discuss the realization of the Ising model on the Sierpiński carpet. In Sec. III the analysis of the static Monte Carlo results and the problems encountered with the finite-size scaling method are presented. Section IV contains the results obtained from the dynamical simulations.

II. SIERPIŃSKI-ISING MODEL

The Sierpiński carpets we use are the smallest possible ones with fourfold symmetry allowing periodic boundary conditions. They are constructed by an iteration process, i.e., starting from an ''initiator'' one replaces all ''substituands'' by the ''generator.''[10,26] As indicated in Fig. 1 the initiator and also the substituand is a gray square and for the generator a 3×3 square with a hole in the center is taken. With the lateral size of the generator l and the size of the hole q the generator consists of l^D-q^D subsquares, that is the generator in Fig. 1 consists of eight gray squares, since the dimension of the embedding space D is two in our case. After k iterations one obtains a structure of lateral size l^k consisting of $s_{lq}(k)=(l^D-q^D)^k$ subsquares. The Hausdorff dimension[26] of this carpet is then $d_{\mathcal{H}}=\ln(l^D-q^D)/\ln(l)$, which is lower than the space dimension $D>d_{\mathcal{H}}$ since $l>q>0$.

For the simulations we consider also an *expanded* Sierpiński lattice. The expanded form is obtained by tiling a square with $l\times l$ Sierpiński carpets of size l^k, which have been generated by k iterations as described. To obtain the same lateral size l^{k+1} as by a further iteration the square for the tiling is $l\times l$ that is of the size of the generator without any hole. In principle the expansion process could be iterated i times and we will denote the Sierpiński carpet as $SC_{lq}(k,i)$ with $i=0$ the nonexpanded form and $k\to\infty$ the fractal in the strict mathematical sense.

The Ising spins are placed on the sites,[20,27] i.e., the center of the filled squares in Fig. 1. One could also put them on the vertices of the lattice[28,29] without changing the Hausdorff dimension and therefore without expecting changes in the critical exponents. The interaction is ferromagnetic and mediated by nearest-neighbor interaction. The Hamiltonian is given by

$$H=-J\sum_{(ij)}\mathbf{S_i}\cdot\mathbf{S_j} \tag{1}$$

with J positive and $\mathbf{S_i}\in\{-1,1\}$ classical Ising spins. The sum is over all nearest-neighbor spin pairs. The average number of nearest neighbors for the lattice $SC_{lq}(k,i)$ is

$$\overline{n}_{ki}=4-4q\frac{1-l^k/(l^2-q^2)^k}{(l^2-q^2)-l} \tag{2}$$

periodic boundary conditions included. This number does not change if the lattice is expanded, i.e., it does not depend on the number i of the expansions.

III. STATIC CRITICAL BEHAVIOR

The low-temperature phase (LTP) below the critical temperature T_c and the high-temperature phase (HTP) above are studied avoiding the finite-size scaling (FSS) method. We will demonstrate why the traditional FSS method cannot be used to extract the critical properties of magnetic systems on fractal lattices.

A. Algorithms, quantities, and errors

For the simulation we use cluster algorithms[30,31] since they have been proved to be more efficient than local algorithms like the Metropolis or heat-bath method.[30–33] Indeed they allow to cross the phase space in larger steps, by flipping at once a large number spins. Thereby the correlation time is reduced and a larger number of independent samples is produced with the same numerical effort. With this advantage and the fact that we can now use a larger number of Monte Carlo (MC) steps we can reduce the statistical errors for the exponents at least by one order of magnitude compared to the previous studies in the 1980s.[19,34]

The choice between the Swendsen-Wang algorithm (SWA) and the Wolff algorithm (WA) for the HTP or LTP region is decided the following way. The Wolff algorithm (WA) is derived from the algorithm of Swendsen and Wang (SWA) and both are cluster algorithms. The SWA divides the entire lattice into clusters, where the probability to connect two sites o and j along a specific link is with the reciprocal of the temperature β

$$P=1-\exp(\min\{0,-2J\beta\mathbf{S}_o\cdot\mathbf{S}_j\}), \tag{3}$$

which means, in the case of Ising spins, that all clusters consist of spins pointing in the same direction. A specific spin $\mathbf{S}_j$ pointing in the appropriate direction gets ''a connection'' to a neighboring cluster via a neighbor $\mathbf{S}_o$ with probability P. After all possible bonds are visited and thus all clusters are formed, each cluster is flipped separately with probability $\frac{1}{2}$.

The WA forms clusters in exactly the same way but chooses randomly a site and flips the generated cluster with probability 1, leaving all other clusters untouched. Since the method would be very inefficient otherwise, the site is cho-

sen first and then a cluster is created around it. Both methods fulfill the requirements of accessibility and detailed balance.

In our case we find that the correlation CPU time, i.e., the number of Monte Carlo evolution steps to create two independent samples multiplied with the CPU time needed to do one step, was in the HTP 3 times smaller for the SWA than for the WA, while in the LTP this relation is inverted in favor of the WA but less significant. This is understandable since in the LTP domains of spins pointing in the same direction are large. The WA constructs clusters from a random site starting favorably with a spin belonging to a large cluster rather than one from a small one. In the same LTP the SWA produces large clusters also efficiently but in addition also small ones, because the SWA always covers the whole lattice. For lower temperatures these small clusters become smaller and smaller and their importance decreases, while their creation still costs CPU time. Thus it is more efficient to use the WA and that tackles exclusively the largest clusters.

In the HTP the areas of spins pointing in the same direction become smaller with increasing temperature and the WA tends to single-spin-flip behavior, where only a few sites were updated at each Monte Carlo step. This leads to large correlation times and thus higher ''costs.'' By contrast the SWA, since it covers the whole lattice can also deal with smaller clusters of sizes becoming more and more equal.

The quantities calculated are the energy E as average of the Hamiltonian (1) and the magnetization as average of

$$M=\sum_{i=1}^{N} \mathbf{S}_i, \tag{4}$$

where the sum is over all N spins. The susceptibility χ is then given by

$$\chi=\frac{\langle M^2\rangle-\langle M\rangle^2}{NT}. \tag{5}$$

The averages are indicated by $\langle\cdots\rangle$. In the HTP region $\langle M\rangle$ is put to zero. There is no unambiguous way to extract a correlation length ξ directly from the numerical data due to the lack of translational invariance. We come back to this point in the following section.

In all cases we calculate the error by means of the Jackknife estimator.[35] See Appendix A for details, where we describe a method that allows to calculate the errors in the Jackknife scheme without saving all samples. Otherwise the method would be very space consuming, requiring hundreds of megabytes of storage while the method used here reduces the stored files to the size of a few kilobytes, without losing the necessary information.

B. Problems of finite-size scaling method and results

To avoid finite-size corrections, one has to ensure that the correlation length ξ is smaller than the size of the lattice. The original Sierpiński carpet is part of the expanded one, i.e., $SC(k,0)\subset SC(k,1)$, and the number of nearest neighbors are equal, i.e., $\overline{n}_{k,0}=\overline{n}_{k,1}$ (see Sec. II for details). Therefore their thermodynamic behavior must be the same as long as $\xi \ll l_{k,0}$ with $l_{k,0}$ the size of $SC(k,0)$. The expanded carpet

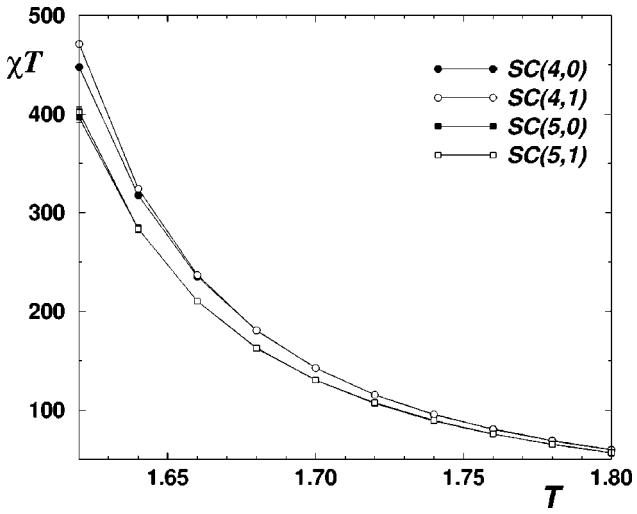

FIG. 2. Behavior of χT in HTP for different lattices. The larger iterated one $SC(5,0)$ does not behave as the original $SC(4,0)$, while the expanded $SC(4,1)$ of $SC(4,0)$ and the expanded $SC(5,1)$ of $SC(5,0)$ do, as long as the correlation length is small enough.

$SC(k,1)$ consists of a number of lattices, nine in our case, of the simple type $SC(k,0)$. As soon as ξ becomes comparable to $l_{k,0}$, finite-size scaling sets in and the behavior of $SC(k,0)$ deviates from that of $SC(k,1)$. Thus a deviation of $SC(k,0)$ from the behavior of $SC(k,1)$ gives a clear indication of the violation of the condition $\xi \ll l_{k,0}$. This scheme provides a control of ξ without actually calculating it directly.

Near the critical point, i.e., when $\xi \gg l_{k,0}$, $SC(k,\infty)$ should behave as a two-dimensional (2D) Ising model, since each $SC(k,0)$ subcell can be taken as a single spin like Kadanoff's block spin. This Ising limit we will not analyze.

The other limit further away from the critical temperature outside the finite-size region for the Sierpiński carpet is analyzed by plotting in Fig. 2 the susceptibility χ in HTP region for the fractals $SC(4,0)$ and $SC(5,0)$ together with their expanded versions $SC(4,1)$ and $SC(5,1)$.

While $SC(4,0)$ behaves as $SC(4,1)$ and $SC(5,0)$ as $SC(5,1)$ the susceptibility for $SC(4,0)$ deviates significantly from the one for $SC(5,0)$. This must be due to the difference in structure and in the average number of nearest neighbors (2) of $SC(k,0)$ and $SC(k+1,0)$. In the temperature region with $\xi \ll l_{k,0}$ the Ising model on the Sierpiński carpet $SC(k,0)$ behaves as expected like $SC(k,\infty)$ rather than like $SC(\infty,0)$. Each $SC(k,0)$ represents a new thermodynamic system and $SC(k+1,0)$ cannot be treated as a scaled version of $SC(k,0)$. The differences between the $k=4$ and $k=5$ versions are also linked to a change of the critical temperature T_c^k that already prohibits the use of FSS in the naive sense.

As long as the lattice is critical, but still $\xi \ll l_{k,0}$ we could try a direct fit of the susceptibilities χ or—with another exponent—the magnetization M

$$\chi T=\chi_0|T-T_c|^{-\gamma}(1+\text{correct.}) \tag{6}$$

However, the uncertainty of T_c and the presence of possible corrections make the determination of a precise exponent γ rather difficult. A way around is to use data from LTP and

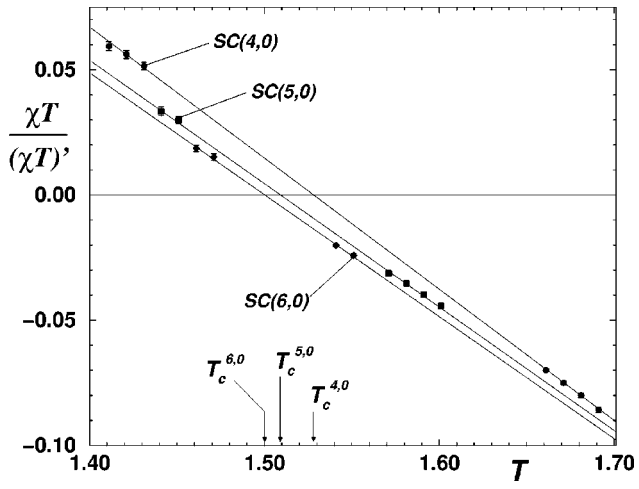

FIG. 3. Results of $\chi T/(\chi T)'$ for different lattices. The slope of the fitted straight line gives the inverse of the critical exponent γ and the intersection with the zero line the critical temperature.

HTP region in the same fit and to ''linearize'' the plot by taking instead of χT the ratio $(\chi T)/(\chi T)'$ with the temperature derivative in the denominator. In order to do this we have to calculate also the derivative of χ or generally of a quantity A making use of

$$\frac{\partial}{\partial T}\langle A\rangle = \beta^2(\langle AE\rangle - \langle A\rangle\langle E\rangle) \tag{7}$$

with $A=M$ or M^2 that introduces higher moments to be determined. In lowest approximation the quotient $\chi T/(\chi T)'$ is the same in LTP and HTP region

$$\frac{\chi T}{(\chi T)'} = -\frac{(T-T_c)}{\gamma}(1+\text{correct.}) \tag{8}$$

and one can determine $1/\gamma$ as the slope of a straight line. We have used this method for the Ising model[36] and found it had principal advantages compared to a direct fit. One has a direct and visual control of the fit and obtains more reliable results. The method also provides implicitly an indicator whether or not the system behaves critical. The straight-line behavior, which can be seen in Fig. 3 sets in only if the system is really critical, but stops as soon as $\xi \ll l_{k,0}$ is violated.

In Fig. 3 only points ''valid'' in this sense are shown. The results differ markedly for different Sierpiński carpets k. Especially the critical temperature, given by the intersection of the fitted line with the x axis, decreases with k, which corresponds to a decreasing average number of nearest neighbors $\overline{n_k}$ (2) if the iteration depth increases. Also the slope $1/\gamma$ changes, fortunately not so strong, see Table I. It is not clear how one could extrapolate to the limit $k\to\infty$, since already $SC(6,0)$ with 2^{18} spins could not be checked by the expanded lattices $SC(6,1)$ with nine times more spins. In all cases for equilibration 10^5 MC steps were used and 10^6 steps to obtain sufficient statistics.

The numerical results obtained from the straight line fits are listed in Table I. The points in Fig. 3 are not distributed symmetrically around T_c and this is not optimal for the fit. Moreover the LTP critical region is very narrow, where the system is not yet in FSS region. Therefore only a small number of points can be used. This leads to a loss in accuracy and we could not complete the entries for $SC(6,0)$ in Table I.

From Figs. 2 and 3 and from the variation of $T_c(k)$ in Table I it is obvious that a straight forward application of the FSS method is impossible. The basic idea behind FSS can be summarized by the following equation, valid for χ and also for other thermodynamic quantities by changing the first exponent,

$$\chi(T) = L^{\gamma/\nu} f((T-T_c)L^{1/\nu}) \tag{9}$$

which states, that χ is a generalized homogeneous function in L. At T_c Eq. (9) simplifies to $\chi(T_c)\propto L^{\gamma/\nu}$. The ratio of critical exponents γ/ν is then obtained as slope by plotting $\ln\chi$ as function of $\ln L$. Of course the use of FSS requires the availability of large and many different realizations of the *same* system. However *a priori* it is unknown how to enlarge a Sierpiński carpet; there is no obvious way doing it, since scaling of $SC(k,i)$ in k leads to a different behavior of $SC(k,0)$ and $SC(k+1,0)$ even if the correlation length is sufficiently small, $\xi \ll l_{k,0}$, while scaling in i violates the construction law of the Sierpiński carpet and leads to a usual 2D-Ising behavior. Furthermore FSS can only work out if all the sizes have the same critical temperature, which is not the case for the few Sierpiński lattices $SC(k,0)$ we could analyze. In case of the fractals the number of nearest neighbors $\overline{n}$ varies if the size given by k changes. This has the consequence that apart from the change of T_c in Eq. (9) to T_c^k, one has also to consider a dependence of the scaling function f on k. Elimination of the shift in T_c by using the ''maximum-of-susceptibility'' method to obtain critical exponents would be a doubtful procedure since the unknown variation of f^k enters.

TABLE I. Results from static behavior. Two estimates exist for γ, one from the method referenced as ''slope method'' and in addition from direct fits, which produces also an estimate for β.

Lattice	T_c (slope method)	γ by slope (slope method)	β directly (HTP only)	directly (LTP only)
$SC(4,0)$	1.5266(11)	1.911(15)	1.901(36)[a]	0.1043(9)[a]
$SC(5,0)$	1.5081(12)	2.030(35)	2.069(8)[a]	0.1221(6)[a]
$SC(6,0)$	1.4992(11)	2.055(54)		

[a]Imposing T_c (see text).

TABLE II. Results from dynamic critical behavior.

Lattice	$V_1(t)\rightarrow \nu z$	$\chi(V_1)\rightarrow \gamma$	$M(V_1)\rightarrow \beta$
$SC(4,0)$	3.06(11)	1.959(32)	0.1154(29)
$SC(5,0)$	3.21(15)	2.048(49)	0.1200(55)

These limitations could explain why the exponents found by the FSS method[20] are so different from the exponents of previous studies (see Table III of Ref. 20) and also from our results (see Table I and II). We note that the use of free boundaries in Ref. 20 with additional finite- size corrections could increase the problems with the FSS method.

To obtain the exponents γ and β, as reported in the second and third columns of Table I, we have used the ''slope'' method (8) explained above and direct fits according to Eq. (6) without any correction terms. These fits have been done by fixing the critical temperature at the value determined by the slope method. This way we arrive at the small errors quoted in Table I. With T_c as a free parameter the errors would increase without changing the results considerably. In the LTP region the number of points is too small for a direct fit of χT to Eq. (6) in order to give reliable estimates for the critical exponents. The exponents γ obtained with the two methods agree quite well. We observe a small but systematic growth of the exponent γ as function of the iteration parameter k.

Before we compare the results with the RG predictions[37] we study first the dynamical properties of the system in order to have an independent check.

IV. DYNAMIC CRITICAL BEHAVIOR

A. Algorithm and scaling

In this section we want to study the dynamical behavior of the fractal Ising model at the critical temperature. The method consists of ''annealing'' the spin system from $T=0$ to the critical temperature T_c. As a function of time or evolution steps, the magnetization or another quantity is recorded before the system reaches the equilibrium state. *Prima facie* it is surprising that the system shows critical behavior although it is not in equilibrium. Indeed the study of critical behavior by the dynamic approach has not been very common in numerical simulations. For quite some time, however, it had been shown that between a short time t_0 and a much longer equilibration time t_f there exists a period where the calculation of the critical properties should be feasible[22–24] (see a recent review of Zheng.[25])

The dynamic critical behavior is similar to the normal critical behavior in the sense that in the annealing process after the time t_0 a finite correlation length ξ exists that grows steadily until it reaches the system size at t_f. In essence this is equivalent to the increase of correlation length in approaching T_c until the FSS region is reached. For $t<t_f$ one observes critical behavior in the form of a power law as in Fig. 4. The critical exponents one obtains are free from finite-size corrections since $\xi<L$.

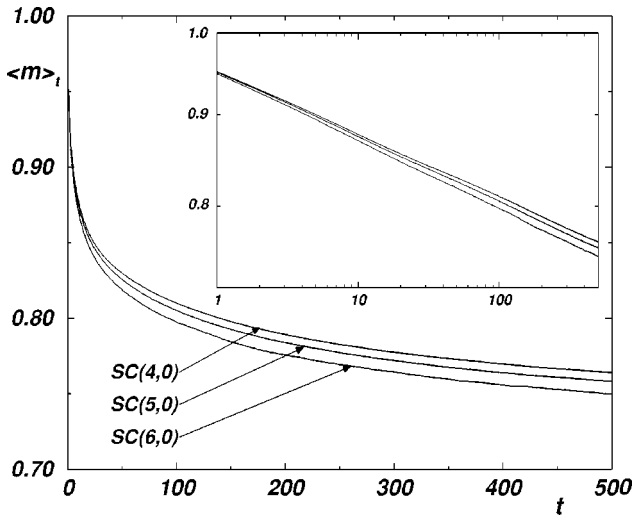

FIG. 4. The average magnetization $\langle m\rangle_t=\langle M\rangle_t/N$ after t evolution steps for different lattices.

We reformulate the results of Ref. 25 for our purposes. One assumes that the free energy per site f has the usual scaling form

$$f((T-T_c),h,t)=b^{-d}f((T-T_c)b^{y_t},hb^{y_h},t/b^z) \quad (10)$$

with the time t measured in MC steps and the dynamical exponent z included. The magnetic field is denoted by h and d the dimension. While FSS is impossible since it is not known how to scale the *size* of the system systematically without changing relevant properties, the dynamics can be assumed to obey the usual scaling since scaling of *time* is not affected by the lattice structure, as time is measured and scaled in number of Monte Carlo steps. However we note that assuming the resulting exponents of the dynamic approach to be estimates of exponents of the thermodynamic limit, without knowing how to scale size, i.e., how to construct this limit, raises an interesting philosophical question about the meaning of such estimates. We expect them to approximate the exponents of $SC(\infty,0)$ better and better with each step of iteration of k in $SC(k,0)$.

In Eq. (10) the part of the free energy that is analytical near T_c has been dropped. The exponents y_t and y_h are the usual ones given by[38]

$$y_t=1/\nu, \quad (11)$$

$$y_h=d-\beta/\nu=(d+\gamma/\nu)/2, \quad (12)$$

with the Josephson relation $2\beta+\gamma=d\nu$ automatically satisfied.

Assuming that the various thermodynamic quantities as obtained by deriving Eq. (10) correspond to their averages after time t, $\langle\rangle_t$, the spontaneous magnetization is

$$\langle M\rangle_t=\left.\frac{\partial f}{\partial h}\right|_{h=0}=b^{-d+y_h}f_h((T-T_c)b^{y_t},0,t/b^z), \quad (13)$$

where f_h is the derivative with respect to h. Using Eqs. (11) and (12) and putting $b=t^{1/z}$ one gets

$$\langle M\rangle_t = t^{-\beta/(z\nu)} f_h((T-T_c)t^{1/(z\nu)},0,1), \tag{14}$$

which reduces at $T=T_c$ to

$$\langle M\rangle_t \propto t^{-\beta/(z\nu)}. \tag{15}$$

In the same way one finds at the critical temperature

$$\chi_t = \left.\frac{\partial^2 f}{\partial h^2}\right|_{h=0} \propto t^{\gamma/(z\nu)}, \tag{16}$$

$$U_t = 1 - \frac{\langle M^2\rangle_t}{\langle M\rangle_t^2} \propto t^{d/z}, \tag{17}$$

$$V_{1t} = \left.\frac{\partial \ln(\langle M\rangle_t)}{\partial T}\right|_{h=0} \propto t^{1/(z\nu)}, \tag{18}$$

from the definition of the susceptibility χ, the time-dependent equivalent to Binder's parameter[39] U or the cumulant V_1. All these formulas can be written as the usual FSS power laws like Eq. (9) with the substitution $t^{1/z} \to L$. In the following section we will use these relations to determine the critical exponents.

B. Simulations

The lattice is prepared in the ferromagnetic ground state, which corresponds to $T=0$. Then the system is exposed to 500 heat-bath steps using the temperature T_c, where a full lattice update is counted as one time step. This procedure must be repeated many times and with 2×10^4 repetitions enough statistical reliability is obtained. For T_c we have taken the value determined by the method given above (see Table I). Therefore we have at least two sources for the errors. One due to the statistical errors (see Appendix B) and one due to the error on T_c.

Besides the averages of the energy $\langle E\rangle_t = \langle H\rangle_t$ Eq. (1), magnetization $\langle M\rangle_t$ Eq. (4) and susceptibility $\chi(t)$, see Eq. (5), the following thermodynamic quantities are determined

$$V_{1t} = \frac{\langle ME\rangle_t}{\langle M\rangle_t} - \langle E\rangle_t, \tag{19}$$

where $\langle \ldots \rangle_t$ denotes the average over different runs (here 2×10^4) after the same number of updating steps t (here $1 \leqslant t \leqslant 500$).

C. Results

In Fig 4 we have plotted $\langle m\rangle_t$ as function of time t, which is the number of evolution steps of the heat bath algorithm. From the slope of a double log plot of the curve and Eq. (14) the ratio of critical exponents $\beta/\nu z$ could be obtained.

However, it is more efficient to determine β directly by drawing $\langle m\rangle_t$ against V_{1t} (Fig. 5) in a double log plot and using a linear fit. The results for the first t_0 steps of the evolution show not yet critical behavior. Since t_0 is *a priori* unknown the fit is applied to different ranges $[t_i < t_{i+1}]$ of data. As soon as linear behavior sets in, this determines t_0 as an upper boundary and a fit can be applied to the entire range

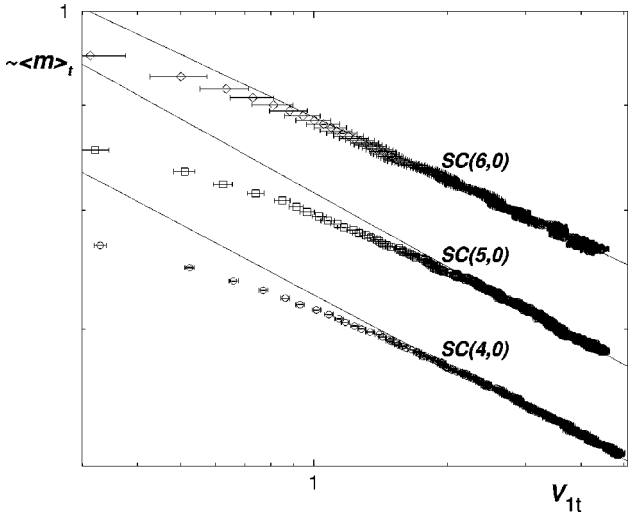

FIG. 5. Magnetization $\langle m\rangle_t$ versus V_{1t} in a double-logarithmic plot giving β as the slope. The results of $SC(5,0)$ $[SC(4,0)]$ are shifted downwards by a factor 0.9 [0.81].

$(t_0,500)$. For $SC(4,0)$ t_0 was $\leqslant 80$ and $\leqslant 100$ for the Sierpiński carpets $SC(5,0)$ and $SC(6,0)$. We have verified that a similar behavior is obtained using the Metropolis algorithm instead of the heat-bath algorithm. The initial time t_0 is longer, in agreement with the observation for the Ising model on the square lattice.[25]

Similarly we obtain the exponents γ and νz, plotting χ_t as function of V_{1t} (Fig. 6) and V_{1t} as function of t (Fig. 7). All results are listed in Table II for the $SC(4,0)$ and $SC(5,0)$. The typical statistical error of exponents found in a double log fit at a given temperature is one-half or more of the overall error. Another important source of uncertainty is as expected the limited accuracy of the critical temperature. To take into account the uncertainty of T_c, we have simulated the system at three different temperatures, at T_c and at $T_c \pm \sigma$, where σ is one standard deviation of T_c. Due to limited

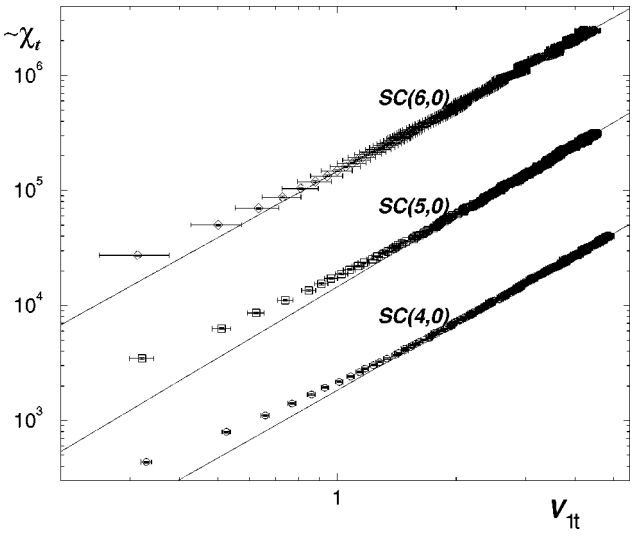

FIG. 6. Susceptibility χ_t versus V_{1t} in a double-logarithmic plot giving γ as the slope.

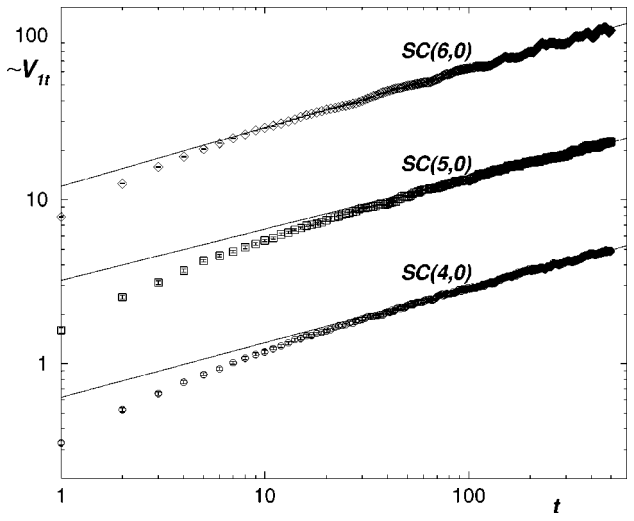

FIG. 7. V_{1t} versus the number of Monte Carlo steps t as double-logarithmic plot giving $1/(\nu z)$ as the slope. The results of $SC(6,0)$ $[SC(5,0)]$ are shifted upwards by a factor 25 [5].

computing resources it was not possible to calculate reliable estimates for exponents and their uncertainties of $SC(6,0)$.

Both methods, the equilibrium as well as the dynamic critical behavior, involve only two independent static critical exponents: γ and β are given by both methods, while the second gives in addition the dynamic critical exponent νz. The results for β and γ from the dynamic simulations compare favorably with those of the static simulations.

V. CONCLUSION

We have studied the phase transition of the Ising model on the Sierpiński carpet of type $3-1$. To obtain consistent results we avoided the finite-size scaling method that we think cannot be used to study magnetic phase transitions on fractal lattices. We used two different methods, the first based on standard simulation techniques and the other based on critical dynamics. Applying it to fractals we give a further example of its practicality. Both methods lead to consistent results that indicate a significant deviation from 2D-Ising behavior. This gives a further evidence that fractal lattice possess a fractal, that is noninteger dimension also in the sense and context of critical phenomena. This result is probably more important than the precise values of the critical exponents.

In conclusion we compare our results with the RG calculations[37] with the Hausdorff dimensions of our Sierpiński carpet $d=1.893$, the $4-\epsilon$ RG gives $\gamma\approx 1.85$ and $\beta \approx 0.10$. The results that we get, $\gamma\approx 2.05$ and $\beta\approx 0.12$, would be more compatible with $d\approx 1.70$. A mean-field-like explanation for this smaller value is that the coordination number of $\overline{n}_\infty=3.2$ suggests $d=\overline{n}_\infty/2=1.6$.[34] Although we cannot exclude other corrections that could cause these deviations, our results suggest that the Hausdorff dimension of the lattice is not exactly the effective noninteger spatial dimension for the phase transition even if it should give a rough estimate.

After completion of this manuscript, the authors became aware of a paper by Zheng and Li[40] that investigates, independently, the short-time critical dynamics of an Ising system on a Sierpiński carpet, partly by means of FSS. However, differences at least for all nonuniversal quantities are expected, since in Ref. 40 the spins have been placed at the vertices, rather than at the sites.

ACKNOWLEDGMENTS

This work was supported by the Alexander von Humboldt Foundation. We thank P.-Y. Hsiao, P. Monceau, and M. Perreau for interesting discussions.

APPENDIX A: CALCULATION OF ERRORS FOR THE EQUILIBRIUM PROPERTIES

We used the so-called Jackknife estimator, which is a special case of resampling, to calculate the average values and the errors, see Ref. 35. The usual way to apply this method is to store the entire sample during the MC simulation (which means the values of M and E after each sweep here) and to calculate the required quantities of all subsamples thereafter. Huge volumes of data, in our simulation 20 MB, have to be stored for each point and reprocessed for each required quantity. To avoid this overhead, we express the Jackknife estimators for functions of expectation values $\langle f\rangle_J$ and their standard deviation $s^2(f)_J$ by simple averages. For $f(x)=x$ we obtain

$$\langle x\rangle_J=\tilde{x} \tag{A1}$$

$$s^2(x)_J=\frac{1}{(N-1)}(\widetilde{x^2}-\tilde{x}^2) \tag{A2}$$

where $\tilde{x}$ denotes the average simply calculated as $\tilde{x}=\Sigma_i x_i/N_{tot}$, where x_i is the value of the quantity in the ith element of the sample and N_{tot} is the size of the sample. N, the number of *independent* elements in the sample, is calculated as $N=N_{tot}/(2\tau+1)$, Ref. 41, with τ the correlation time.

For $f(x)=x^2$ we obtain

$$\langle x^2\rangle_J=\tilde{x}^2+\frac{\widetilde{x^2}-\tilde{x}^2}{(N-1)^2}, \tag{A3}$$

$$s^2(x^2)_J=\frac{1}{(N-1)^3}(-4N^2\tilde{x}^4+4(N+1)N\tilde{x}^2\widetilde{x^2}-4N\tilde{x}\widetilde{x^3} +\widetilde{x^4}), \tag{A4}$$

where we have used $\widetilde{x^n}=\Sigma_i x_i^n/N_{tot}$. For $f(x,y)=x^2+y$, as required for $\chi T=\langle M^2\rangle-\langle M\rangle^2$, where $x=\langle M\rangle$, $y=-\langle M^2\rangle$ and $\chi T=-f(x,y)$

$$\langle x^2+y\rangle_J=\langle x^2\rangle_J+\langle y\rangle_J, \tag{A5}$$

$$s^2(x^2+y)_J=\frac{4N}{(N-1)^2}(\widetilde{x^2}\tilde{y}-\tilde{x}\widetilde{xy})+\frac{2}{(N-1)^2}(\widetilde{x^2}\tilde{y}-\widetilde{x^2}\tilde{y}), \tag{A6}$$

The denominators in a function $f(x,y)=x/y$ are of course assumed to be nonvanishing. In the following we will treat the estimates of f as well as their standard deviation up to at least $\mathcal{O}(N^{-2})$:

$$\langle x/y\rangle_J=\frac{\widetilde{x}}{\widetilde{y}}\left(1+\frac{1}{N^2}\left[\frac{\widetilde{y^2}}{\widetilde{y}^2}-\frac{\widetilde{xy}}{\widetilde{x}\widetilde{y}}\right]\right)+\mathcal{O}(N^{-3}) \tag{A7}$$

$$s^2(x/y)_J=\frac{N-1}{N^2\widetilde{y}^4}(\widetilde{x^2}\widetilde{y}^2-2\widetilde{x}\widetilde{y}\widetilde{xy}+\widetilde{x}^2\widetilde{y^2})+\mathcal{O}(N^{-2}) \tag{A8}$$

For $f(x,y,z)=x/y+z$ as used for V_1 with $x=\langle ME\rangle$, $y=\langle M\rangle$ and $z=-\langle E\rangle$ we get

$$\langle x/y+z\rangle_J=\langle x/y\rangle_J+\langle z\rangle_J, \tag{A9}$$

$$s^2(x/y+z)_J = s^2(x/y)_J+s^2(z)_J+\frac{2}{N}\left(\frac{\widetilde{xz}}{\widetilde{y}}-\frac{\widetilde{x}\widetilde{yz}}{\widetilde{y}^2}\right)+\mathcal{O}(N^{-2}) \tag{A10}$$

The special cases just discussed can be generalized as follows. The generalization turns out to be very useful and easily implemented. With the functions

$$F(x_1,x_2,\ldots,x_\nu):=\sum_{i_1i_2\cdots i_\nu}a_{i_1i_2\cdots i_\nu}x_1^{i_1}x_2^{i_2}\cdots x_\nu^{i_\nu}, \tag{A11}$$

$$H(x_1,x_2,\ldots,x_\nu):=\sum_{i_1i_2\cdots i_\nu}b_{i_1i_2\cdots i_\nu}x_1^{i_1}x_2^{i_2}\cdots x_\nu^{i_\nu} \tag{A12}$$

that are sums of products of the i_νth powers of observables x_ν, it is a matter of straightforward but tedious algebra to show that

$$\langle F\rangle_J=\widetilde{F}:=F(\widetilde{x_1},\widetilde{x_2},\ldots,\widetilde{x_\nu})+\mathcal{O}(N^{-2}) \tag{A13}$$

$$\left\langle\frac{F}{H}\right\rangle_J=\frac{\widetilde{F}}{\widetilde{H}}+\mathcal{O}(N^{-2}) \tag{A14}$$

where $\widetilde{x_\nu}=\Sigma_i x_{\nu i}N_{tot}$ with $x_{\nu i}$ as the value of observable x_ν obtained at the ith step of the simulation. The standard deviation are given then as

$$s^2(F)_J=\frac{1}{N}\sum_{\substack{i_1i_2\cdots i_\nu\\ i_1'i_2'\cdots i_\nu'}}a_{i_1i_2\cdots i_\nu}a_{i_1'i_2'\cdots i_\nu'}\widetilde{x_1^{(i_1+i_1')}}\widetilde{x_2^{(i_2+i_2')}}\cdots \times\widetilde{x_\nu^{(i_\nu+i_\nu')}}\sum_{\substack{\kappa=1,2,\cdots,\nu\\ \lambda=1,2,\cdots,\nu}}i_\kappa i_\lambda'\frac{\widetilde{x_{i_\kappa}x_{i_\lambda'}}-\widetilde{x_{i_\kappa}}\widetilde{x_{i_\lambda'}}}{\widetilde{x_{i_\kappa}}\widetilde{x_{i_\lambda'}}}+\mathcal{O}(N^{-2}) \tag{A15}$$

$$s^2(F/H)_J=\frac{\widetilde{H}^2s^2(F)_J+\widetilde{F}^2s^2(H)_J}{\widetilde{H}^4} -2\frac{1}{N}\sum_{\substack{i_1i_2\cdots i_\nu\\ i_1'i_2'\cdots i_\nu'}}b_{i_1i_2\cdots i_\nu}a_{i_1'i_2'\cdots i_\nu'} \times\widetilde{x_1^{(i_1+i_1')}}\widetilde{x_2^{(i_2+i_2')}}\cdots\widetilde{x_\nu^{(i_\nu+i_\nu')}} \times\sum_{\substack{\kappa=1,2,\cdots,\nu\\ \lambda=1,2,\cdots,\nu}}i_\kappa i_\lambda'\frac{\widetilde{x_{i_\kappa}x_{i_\lambda'}}-\widetilde{x_{i_\kappa}}\widetilde{x_{i_\lambda'}}}{\widetilde{x_{i_\kappa}}\widetilde{x_{i_\lambda'}}}+\mathcal{O}(N^{-2}) \tag{A16}$$

One constraint that should be always checked is

$$\widetilde{x_ix_i}-\widetilde{x_i}\widetilde{x_i}\geqslant 0.$$

In all cases numerical errors may become important, since small differences of large numbers are treated here.

APPENDIX B: CALCULATION OF ERRORS FOR THE DYNAMICAL PROPERTIES

While the errors of the static properties were calculated in a straightforward manner, dynamic errors are more complex. Correlations coming from the dynamic behavior of the system must be distinguished from correlations due to insufficient sampling. At first glance all dynamic runs are mutually independent, because they are all prepared in the same state in the beginning. Therefore usual error-estimation techniques and thus the following scheme seems to be applicable (this scheme is referenced in the following as the ''direct method''): Collect each configuration Σ_t^i, which was created after t evolution steps in run i, in an ordered set,

$$S_t=\{\Sigma_t^1,\Sigma_t^2,\cdots,\Sigma_t^N\} \tag{B1}$$

where N is the number of runs and $1\leqslant t\leqslant t_{max}$, where t_{max} is the maximal time. For each configuration in each set the properties of interest are calculated. For instance an estimator for the magnetization $\langle M\rangle_t$ at t steps is given by

$$\langle M\rangle_t=\frac{1}{N}\sum_i^N M(\Sigma_t^i). \tag{B2}$$

The standard deviation could also be calculated in the usual way

$$\sigma^2(\langle M\rangle_t)=\frac{1}{N}\sum_i^N[M(\Sigma_t^i)-\langle M\rangle_t]^2. \tag{B3}$$

In more complicated cases, again the Jackknife could be applied and the formulas as given above can be used to calculate an estimator, for example, for V_{1t} and its uncertainty. The logarithms of these data then enter a linear fitting routine and an estimator for the critical exponents, say μ, is computed. Although actually a set of estimates and standard deviations of a property enter the fitting routine, all these details are hidden by writing the linear fitting routine μ as a function of all ordered sets S_t

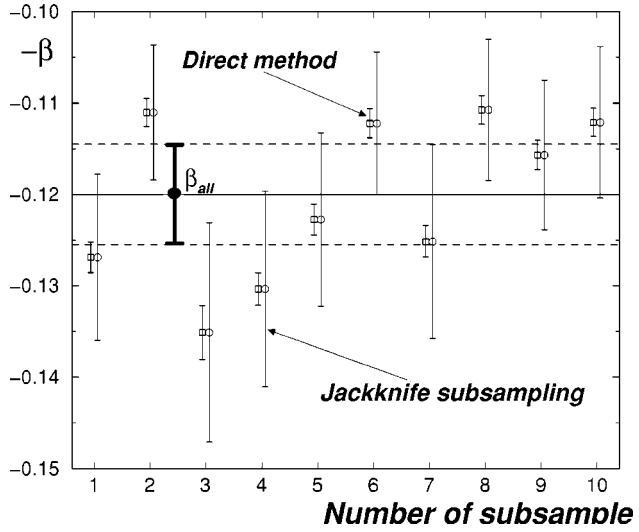

FIG. 8. Comparison of two methods for calculating estimates and errors of exponents for dynamical properties. The direct way leads to incompatible results, while the Jackknife gives reasonable estimates of the errors.

$$\mu = \mu(S_1, S_2, \ldots, S_{t_{max}}). \tag{B4}$$

Unfortunately this simple approach turns out to be wrong: Even though each set S_t consists indeed of mutually independent configurations, the different sets S_t from different times t are not only connected by the dynamic behavior of the system (which is the wanted and investigated behavior that lead to critical exponents at all). They are additionally connected by the naive method they are produced by. ''Naive method'' here refers to the fact, that we create only one subsequent sample at each step instead of considering the entire phase space accessible from any current state. Instead of creating a whole histogram of transitions from one state to another, we create only *one* subsequent state, hoping that this state is a typical one. Apart from this, a rather atypical and thus unimportant representative at a particular time might produce also atypical representatives at subsequent times.

However the subsampling scheme as used by the Jackknife method can again be used to estimate the average and its error in this case. We create new samples, $S_t^{J_i}$ by deleting the configurations of run i from all sets S_t:

$$S_t^{J_i} = \{\Sigma_t^1, \Sigma_t^2, \ldots, \Sigma_t^{i-1}, \Sigma_t^{i+1}, \ldots, \Sigma_t^N\} = S_t \backslash \{\Sigma_t^i\}. \tag{B5}$$

For each of these sets, we calculate our estimate of the critical exponent, $\mu^{J_i} = \mu(S_1^{J_i}, S_2^{J_i}, \ldots, S_{t_{max}}^{J_i})$. The mean value of these estimates of the exponent

$$\mu^J = \frac{1}{N} \sum_i^N \mu^{J_i}, \tag{B6}$$

represents the Jackknife estimator of the exponent, while

$$\sigma^2(\mu^J) = \frac{N-1}{N} \sum_i^N (\mu^{J_i} - \mu^J)^2 \tag{B7}$$

is its standard deviation (note the prefactor $N-1/N$ instead of $1/N-1$, as in the usual calculation of a standard deviation). The actual calculation of each estimate of the exponent, μ^{J_i}, is independent of the subsampling scheme given here. Thus we note just for a better understanding that μ^{J_i} uses by itself the Jackknife technique to calculate the exponent.

In Fig. 8 we show different results obtained by dividing a whole set of data into ten distinct sets and applying both schemes, where $\langle M \rangle_t$ from $SC(5,0)$ serves as an example. As expected both methods give almost exactly the same estimator for the exponent (here β), but different results for the error. By using the Jackknife scheme the scattering of the results for each subset is well compatible with the results for the estimate and the error from the entire set (marked as β_{all}). Manifestly the direct method gives incompatible results. Additionally the error bar calculated for the entire set by means of the direct method is smaller than the numerical error and thus smaller than the line of β_{all}.

*Email address: Gunnar.Pruessner@physik.fu-berlin.de
†Email address: Damien.Loison@physik.fu-berlin.de
‡Email address: Klaus.Dieter.Schotte@physik.fu-berlin.de

[1] R. J. Baxter, *Exactly Solved Models in Statistical Mechanics* (Academic Press, London, 1982).
[2] M. Tissier, B. Delamotte, and D. Mouhanna, Phys. Rev. Lett. **84**, 5208 (2000).
[3] M. A. Novotny, Phys. Rev. Lett. **70**, 109 (1993).
[4] M. A. Novotny, Int. J. Mod. Phys. C **7**, 361 (1996).
[5] D. O'Connor and C. R. Stephens, J. Phys. A **25**, 101 (1992).
[6] D. O'Connor and C. R. Stephens, Nucl. Phys. B **360**, 297 (1991).
[7] M. A. Novotny, Europhys. Lett. **17**, 297 (1992); **18**, 92[E] (1992).
[8] M. A. Novotny, Phys. Rev. B **46**, 2939 (1992).
[9] Y. Gefen, A. Aharony, and B. B. Mandelbrot, J. Phys. A **17**, 1277 (1984).
[10] B. B. Mandelbrot, *The Fractal Geometry of Nature* (Freeman, New York, 1983).
[11] Y. Gefen, B. B. Mandelbrot, and A. Aharony, Phys. Rev. Lett. **45**, 855 (1980).
[12] A. A. Migdal, Zh. Eksp. Teor. Fiz. **69**, 810 (1975) [Sov. Phys. JETP **42**, 413 (1976)].
[13] L. P. Kadanoff, Ann. Phys. (San Diego) **100**, 359 (1976).
[14] B. Lin and Z. R. Yang, J. Phys. A **19**, L49 (1986).
[15] L. Hao and Z. R. Yang, J. Phys. A **20**, 1627 (1987).
[16] Y. kai Wu and B. Hu, Phys. Rev. A **35**, 1404 (1987).
[17] Y. Gefen, Y. Meir, B. B. Mandelbrot, and A. Aharony, Phys. Rev. Lett. **50**, 145 (1983).
[18] B. Bonnier, Y. Leroyer, and C. Meyers, Phys. Rev. B **37**, 5205 (1988).
[19] G. Bhanot, H. Neuberger, and J. A. Shapiro, Phys. Rev. Lett. **53**, 2277 (1984).
[20] P. Monceau, M. Perreau, and F. Hébert, Phys. Rev. B **58**, 6386 (1998).
[21] J. M. Carmona, U. M. B. Marconi, J. J. Ruiz-Lorenzo, and A.

Tarancón, Phys. Rev. B **58**, 14387 (1998).
[22] H. K. Janssen, B. Schaub, and B. Smittmann, Z. Phys. B: Condens. Matter **73**, 539 (1989).
[23] D. A. Huse, Phys. Rev. B **40**, 304 (1989).
[24] K. Humayun and A. Bray, J. Phys. A **24**, 1915 (1991).
[25] B. Zheng, Int. J. Mod. Phys. B **12**, 1419 (1998).
[26] D. Stoyan and H. Stoyan, *Fractals, Random Shapes and Point Fields* (Wiley, Chichester, 1994).
[27] B. Bonnier, Y. Leroyer, and C. Meyers, J. Phys. (Paris) **48**, 553 (1987).
[28] J. C. A. d'Auriac and R. Rammal, J. Phys. A **19**, L655 (1986).
[29] B. Bonnier, Y. Leroyer, and C. Meyers, Phys. Rev. B **40**, 8961 (1989).
[30] R. H. Swendsen and J. S. Wang, Phys. Rev. Lett. **58**, 86 (1987).
[31] U. Wolff, Phys. Rev. Lett. **62**, 361 (1989).
[32] N. Metropolis, A. W. Rosenbluth, M. N. Rosenbluth, A. H. Teller, and E. Teller, J. Chem. Phys. **21**, 1087 (1953).
[33] K. Binder, in *Phase Transition and Critical Phenomena*, edited by C. Domb and M. S. Green (Academic Press, London, 1976), Vol. 5B, pp. 1–105.
[34] G. Bhanot, D. Duke, and R. Salvador, Phys. Lett. **165B**, 355 (1985).
[35] B. Efron, *The Jackknife, the Bootstrap and Other Resampling Plans* (SIAM, Philadelphia, 1982).
[36] G. Pruessner, D. Loison, and K.-D. Schotte, Physica A **286**, 292 (2000).
[37] J. C. LeGuillou and J. Zinn-Justin, J. Phys. (Paris) **48**, 19 (1987).
[38] J. Cardy, *Scaling and Renormalization in Statistical Physics* (Cambridge University Press, Cambridge, 1997).
[39] K. Binder, Z. Phys. B: Condens. Matter **43**, 119 (1981).
[40] G.-P. Zheng and M. Li, Phys. Rev. E **62**, 6253 (2000).
[41] H. Müller-Krumbhaar and K. Binder, J. Stat. Phys. **8**, 1 (1973).